A Compact Finite-Difference Frequency-Domain Method for Analysis of Microwave Transmission Lines with Rough Surface

Binke Huang and Xubing Wang

Department of Information and Telecommunication Engineering
Xi'an Jiaotong University, Xi'an 710049, China
bkhuang@mail.xjtu.edu.cn

Abstract ─ Accurate modeling of microwave transmission lines is very important in microwave communication and radar systems, especially at high frequencies. A compact finite-difference frequency-domain method (FDFD) is presented to analyze the propagation characteristics of microwave transmission lines with rough conductor surface. Equations in the Maxwell system are discretized with difference method in the cross-section of the microwave transmission line, and rough surface of microwave transmission lines is replaced by complex surface impedance from the conductivity Gradient Model. The eigen equations of the electromagnetic field components are formed and solved to obtain the propagation constants for a given frequency. The presented method reduces the computer storage effectively in ensuring simulation accuracy without the direct modeling for surface roughness, which can be applied in the modeling of complex microwave circuits.

Index Terms ─ Conductor surface roughness, Finite-Difference Frequency-Domain (FDFD), surface impedance boundary conditions, transmission lines.

I. INTRODUCTION

The surface roughness is necessary in manufacture to add the adhesion between the conductor trace and dielectric substrate for planar transmission lines, which will increase transmission loss further. Therefore, accurate characterization the effect of surface roughness in microwave transmission lines is beneficial in analysis and design of microwave circuits, in particular at high frequencies, such as in millimeter waves.

In 1993, Detlev Hollmann computed the transmission loss in full-waves with finite-difference time-domain (FDTD) method [1], and the conductor loss as well as the loss from the conductor rough surface are considered. The FDTD approaches required large memory space and high CPU time, and the phase constants need to be set as an input parameter and the eigen frequencies of interest need to be found via discrete Fourier transform. A 2-D full-wave finite-difference frequency-domain (FDFD) method combined with the surface impedance boundary condition has been applied for the analysis of dispersion characteristics of lossy metal waveguides [2],[3]. For quasi-TEM applications to a wide variety of transmission line structures, a FDFD solver provides an efficient solution for conductor current distributions involving both skin effect and proximity effect [4]. However, all the six field components need to be calculated to yield an eigenvalue equation. Other than the FDFD method which uses a six field matrix, the compact 2-D full-wave finite-difference frequency-domain method is much more efficient to calculate the propagation constants of microwave transmission lines [5],[6], which only involves four transverse field components.

A compact 2-D finite difference frequency domain with surface impedance boundary condition has been applied to analyze the propagation characteristics of surface smooth conductor with finite conductivity [7],[8], however, the propagation characteristics of microwave transmission line with rough surface has not been demonstrated accurately yet. In this paper, a compact finite-difference frequency-domain approach combined with a complex surface impedance of the conductivity Gradient Model is presented to analyze the propagation characteristics of waveguide and microstrip line with rough conductor surfaces.

II. THEORIES

A. Surface impedance for rough surface

For a rough surface in *y*-*z*-plane, a continuous transition of macroscopic conductivity $\sigma(x)$ from 0 to σ_{bulk} perpendicular to the surface can be utilized to model surface roughness in the Gradient Model [9]. Taking this Gradient Model approach, the field distributions and the skin effect in rough conductor surfaces can be deduced from Maxwell's equation with the location dependent conductivity, and this results in a differential equation in one dimension for magnetic field component $B_y(x)$ only [10]. Without loss of generality, the solution for the magnetic field B_y distribution for a given RMS-roughness R_q=1μm and a frequency f=1GHz is shown in Fig. 1 in comparison to the magnetic field for an ideally

Submitted On: December 29, 2018
Accepted On: July 10, 2019

smooth surface at position x=0. Moreover, the current density distribution $J_z(x)$ can be calculated from $B_y(x)$ using Ampère's law. The magnitude of the current density for a rough surface and a perfect smooth surface are also shown in Fig. 1. The current density shows an abrupt step to its maximum value and declines in the conductor for a smooth surface, while the current density for a rough surface delivers a smooth response between dielectric and conductor [11].

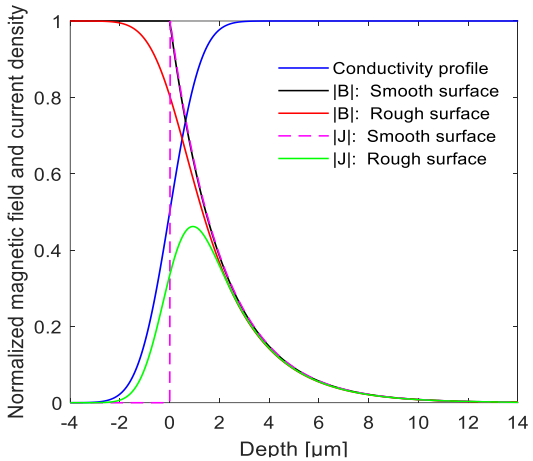

Fig. 1. Magnitude of magnetic field and current density for an ideal smooth surface and a rough surface.

The surface impedance with smooth non-ideal conductor is [12]:

$$Z_{\text{smooth}} = R_s + jX_s = -\mu_0 \frac{E_z}{B_y} = \frac{1+j}{\sigma\delta}, \tag{1}$$

where σ and δ are the intrinsic conductivity and skin-effect depth, respectively. We can see from (1) that $X_s = R_s$ for conductors with smooth surface, as B_y and J_z show the same x-dependency in Fig. 1.

For conductor with rough surface, however, real and imaginary part will not be equal ($X_s \neq R_s$), as B_y and J_z do not show the same x-dependency (Fig. 1). The ratio of E_z and B_y in (1) must therefore be expressed by the responses of B_y and J_z obtained with the conductivity Gradient Model [11].

With the Maxwell equations, we have:

$$(\nabla \times \bar{E})_y = -\frac{\partial E_z}{\partial x} = -j\omega B_y \rightarrow E_z = j\omega \int B_y dx, \tag{2}$$

$$(\nabla \times \bar{B})_z = \frac{\partial B_y}{\partial x} = \mu_0 J_z \rightarrow B_y = \mu_0 \int J_z dx. \tag{3}$$

The surface impedance for conductor with rough surface can be derived directly [11]:

$$Z_{\text{rough}} = -j\omega \frac{\int B_y dx}{\int J_z dx}. \tag{4}$$

Figure 2 shows typical frequency responses of its real and imaginary part in comparison to those of a smooth surface.

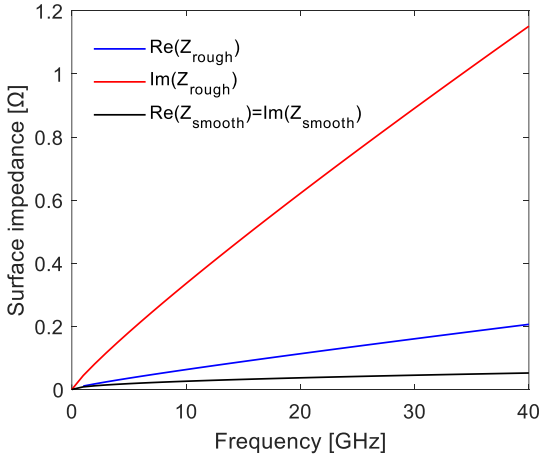

Fig. 2. Real and imaginary part of the surface impedance of copper for a rough surface with 1um RMS-roughness and a smooth surface.

With a series derivation for B_y and J_z [13], the surface impedance condition with rough conductor surface can be obtained, which can be convenient incorporated into conductor boundary condition in the FDFD method to characterize the effects of rough surface for microwave transmission lines.

B. A compact 2-D full-wave finite-difference frequency-domain method

Inside the transmission lines, the transverse field components can be expressed by eliminating the longitudinal components from the Maxwell curl discrete equation as follows [5]:

$$\begin{aligned} &-j\frac{\gamma}{k}E_x(i,j) \\ &= -\frac{1}{k^2\Delta x\Delta y}[H_x(i,j-1)] - H_x(i+1,j-1) - H_x(i,j) + H_x(i+1,j)] \\ &+ \frac{1}{k^2\Delta x^2}H_y(i-1,j) + (1-\frac{2}{k^2\Delta x^2})H_y(i,j) + \frac{1}{k^2\Delta x^2}H_y(i+1,j), \end{aligned} \tag{5a}$$

$$\begin{aligned} &-j\frac{\gamma}{k}E_y(i,j) \\ &= \frac{1}{k^2\Delta x\Delta y}[H_y(i-1,j)] - H_y(i-1,j+1) - H_y(i,j) + H_y(i,j+1)] \\ &- \frac{1}{k^2\Delta y^2}H_x(i,j-1) - (1-\frac{2}{k^2\Delta y^2})H_x(i,j) - \frac{1}{k^2\Delta y^2}H_x(i,j+1), \end{aligned} \tag{5b}$$

$$\begin{aligned} &-j\frac{\gamma}{k}H_x(i,j) \\ &= \frac{1}{k^2\Delta x\Delta y}[E_x(i-1,j)] - E_x(i-1,j+1) - E_x(i,j) + E_x(i,j+1)] \\ &- \frac{1}{k^2\Delta x^2}E_y(i-1,j) - (1-\frac{2}{k^2\Delta x^2})E_y(i,j) - \frac{1}{k^2\Delta x^2}E_y(i+1,j), \end{aligned} \tag{5c}$$

$$-j\frac{\gamma}{k}H_y(i,j)$$
$$=-\frac{1}{k^2\Delta x\Delta y}[E_y(i,j-1)]-E_y(i+1,j-1)-E_y(i,j)+E_y(i+1,j)]$$
$$+\frac{1}{k^2\Delta y^2}E_x(i,j-1)+(1-\frac{2}{k^2\Delta y^2})E_x(i,j)+\frac{1}{k^2\Delta y^2}E_x(i,j+1), \quad (5d)$$

where γ is the propagation constant and k is the wave number in the free space, Δx and Δy are the mesh sizes in x- and y-direction, respectively.

Equation (5) shows that one component of E (or H) field can be represented by seven components of neighbor H (or E) field. Equation (5) is not applicable to deal the components on the non-ideal conductor boundary. The fields on the boundary must be computed with special boundary conditions.

Considering the finite conductivity of non-ideal conductor, the relationship between the tangential electric field and the tangential magnetic field on the boundary is related with the surface impedance boundary conditions (SIBCs):

$$\bar{E}_{\tan}=Z_s\hat{n}\times\bar{H}_{\tan}. \quad (6)$$

For conductor with smooth surface, the surface impedance Z_s is determined through formula (1). If at high frequencies, the conductor surface roughness need to be considered, the surface impedance for rough surfaces can be calculated with formula (4).

With the SIBCs and eliminating the longitudinal components from the applied Maxwell discrete equations, as shown in Fig. 3 (a), $E_x(i,j)$, $E_y(i,j)$ and $H_y(i,j)$ on the lower boundary satisfy the following formula:

$$-j\frac{\gamma}{k}E_x(i,1)=j\frac{Z_s}{k\Delta x}H_x(i,1)-j\frac{Z_s}{k\Delta x}H_x(i+1,1)$$
$$+j\frac{Z_s}{k\Delta y}H_y(i,1)-j\frac{Z_s}{k\Delta y}H_y(i,2), \quad (7a)$$

$$-j\frac{\gamma}{k}E_y(i,1)$$
$$=(j\frac{Z_s}{k\Delta y}-1+\frac{1}{k^2\Delta y^2})H_x(i,1)+\frac{1}{k^2\Delta y^2}H_x(i,2) \quad (7b)$$
$$-\frac{1}{k^2\Delta x\Delta y}H_y(i-1,2)+\frac{1}{k^2\Delta x\Delta y}H_y(i,2),$$

$$-j\frac{\gamma}{k}H_y(i,1)=\frac{-jZ_s}{k\Delta y-jZ_S}[-j\frac{\gamma}{k}H_y(i,2)]. \quad (7c)$$

In Fig. 3 (b), applying the SIBC on the left boundary with the non-ideal conductor, we have:

$$-j\frac{\gamma}{k}E_x(1,j)$$
$$=\frac{1}{k^2\Delta x\Delta y}H_x(2,j-1)-\frac{1}{k^2\Delta x\Delta y}H_x(2,j) \quad (8a)$$
$$+(1-\frac{1}{k^2\Delta x^2}-j\frac{Z_s}{k\Delta x})H_y(1,j)+\frac{1}{k^2\Delta x^2}H_y(2,j),$$

$$-j\frac{\gamma}{k}E_y(1,j)=-j\frac{Z_s}{k\Delta x}H_x(1,j)+j\frac{Z_s}{k\Delta x}H_x(2,j)$$
$$-j\frac{Z_s}{k\Delta y}H_y(1,j)+j\frac{Z_s}{k\Delta y}H_y(1,j+1), \quad (8b)$$

$$-j\frac{\gamma}{k}H_x(1,j)=\frac{-jZ_s}{k\Delta x-jZ_S}[-j\frac{\gamma}{k}H_x(2,j)]. \quad (8c)$$

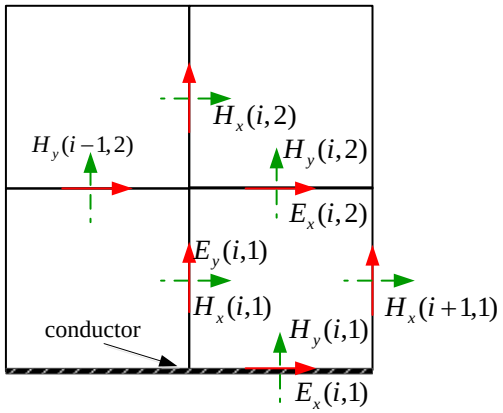

(a)

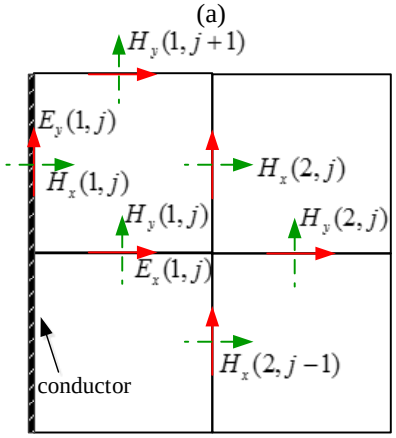

(b)

Fig. 3. Transverse field components on boundary surface: (a) E_x, E_y, and H_y on lower boundary, and (b) E_x, E_y, and H_x on left boundary.

Similarly, the field components on the top boundary and the right boundary can be obtained by applying the SIBCs directly.

From the equations for inner nodes and surface nodes, we can conclude an eigenvalue problem as:

$$[A][X]=\lambda[X], \quad (9)$$

where $[X]=[E_x,E_y,H_x,H_y]^T$, $\lambda=-j\frac{\gamma}{k}=\frac{\beta-j\alpha}{k}$, β is the phase constant, and α is the attenuation constant caused by the mental loss. $[A]$ is a sparse coefficient matrix, and the eigen solution of $[A]$ delivers the propagation constant.

III. NUMERICAL RESULTS

In this section, a waveguide and a shielded microstrip line are provided to illustrate the efficiency of the proposed method.

A. Waveguide

With the FDFD method, the propagation constants for waveguide in different frequencies can be obtained. The waveguide is an empty rectangular copper waveguide with the size of $a \times b$=19.05mm×9mm, and with the conductivity σ=5.8×10^{7}S/m. The computational domain for the cross section of waveguide comprises a grid of 10×5 cells in the FDFD simulation. The computed results of propagation constant for TE_{10} mode of waveguide with smooth surface are compared with the analytical perturbation method [12] with good correction as shown in Fig. 4.

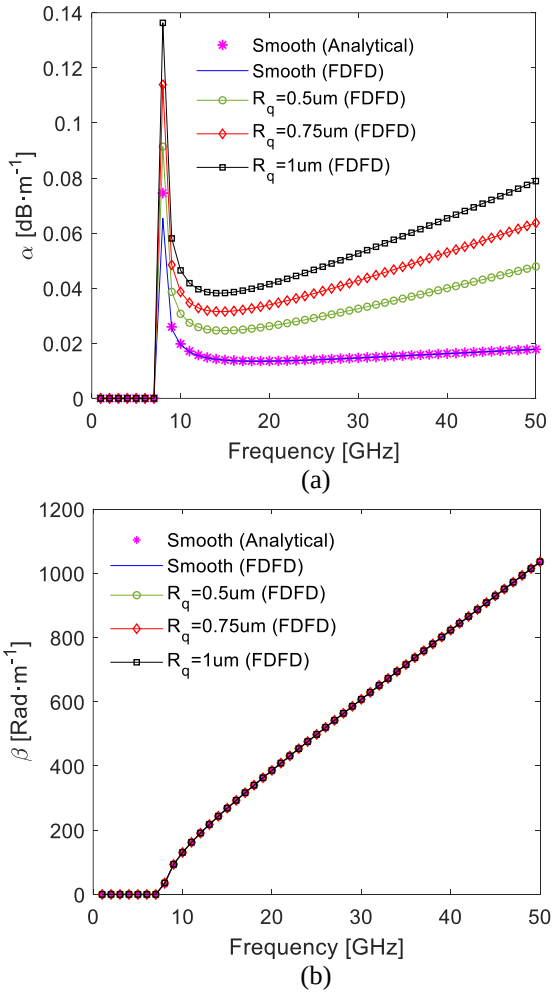

Fig. 4. The propagation of waveguide considering conductor surface roughness: (a) attenuation constant, and (b) phase constant.

As shown in Fig. 4 (a), under other parameters invariably, attenuation constant tends to 0 when the frequency is below cutoff frequency, and as the frequency increases, attenuation constant keeps decreasing in the cutoff region when f tends to f_{min} [14]. The surface impedance is dominant when $f > f_{min}$, so attenuation constant increases as frequency increases. Under other parameters invariably, the attenuation constant monotonically rises as the surface roughness increases in Fig. 4 (a). As shown in Fig. 4 (b), the differences between phase constants of waveguide with smooth surface and roughness surface are negligible.

B. Shielded microstrip line

Consider a shielded microstrip line as defined in Fig. 5 with a trace width w=3.81mm on top of a dielectric layer with ε_r=2.2, tanδ=0, and the height h=2.7mm. The conductor of trace and ground plane is with a conductivity σ=5.8×10^{7}S/m and the thickness is negligible. The width and height for the shielded metallic box are a=9.525mm and b=4.5mm, respectively. The cross section of the shielded microstrip line is meshed with total 10×5 cells in the FDFD simulation. The computed results obtained by our proposed method are given in Fig. 6. Numerical results of propagation constant of microstrip line with smooth surface are compared with the results of CST Microwave Studio and a good agreement is achieved. Under other parameters invariably, the attenuation constant monotonically rises as the frequency increases in Fig. 6 (a), and the roughness of surface increases from 0 to 1um, the value of attenuation constants increase, especially at higher frequencies. As shown in Fig. 6 (b), the differences between phase constant of shielded microstrip with line smooth surface and roughness surfaces are too small to be distinguished.

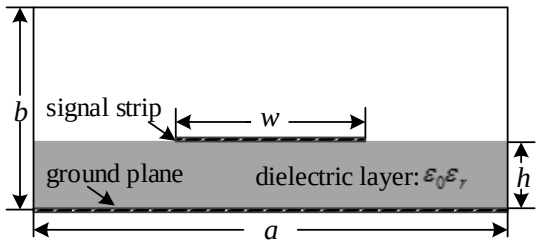

Fig. 5. The cross section of a shielded microstrip line.

Compared to the 2-D FDFD with six components in [3], the dimension of the coefficient matrix [A] in (9) is reduced to two thirds, because only four transverse field components are contained in the compact 2-D FDFD. The comparison of efficiency in calculation the propagation constants for the shielded microstrip line [Fig. 5] are shown in Table 1. The calculations are carried out on Intel (R) I7 2.7GHz laptop using Matlab R2017b.

We can see that the CPU time can be reduced considerably as compared to the case in which six field components are comprised, since the cutting down order of the coefficient matrix largely for solving the eigenvalue problem in the proposed method.

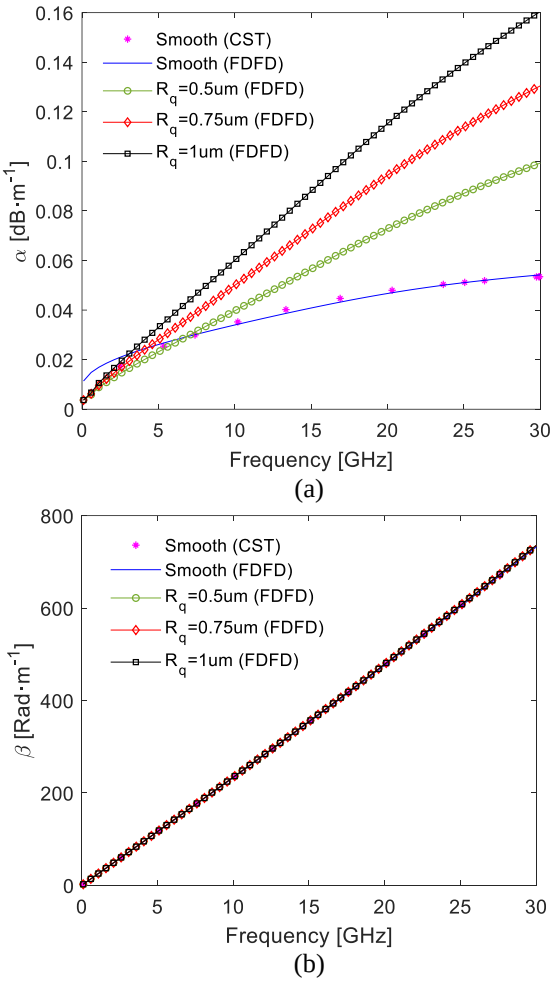

Fig. 6. The propagation of a shielded microstrip line considering conductor surface roughness: (a) attenuation constant, and (b) phase constant.

Table 1: Comparison of this method and the method in [3] for the second example

	This Method	Method in [3]
Dimension of matrix	236	354
Number of non-zero elements	1222	883
CPU time (s)	1.54	6.40

IV. CONCLUSION

In the paper, a compact 2D full-wave FDFD method combined with complex surface impedance of the conductivity Gradient Model has been applied for the dispersion characteristics of microwave transmission lines with roughness surface. Accurate results of attenuation constants and phase constants of waveguide and shielded microstrip line with roughness surface have been obtained by using the proposed method. The proposed method will be a powerful tool to calculate the propagation constants for microwave transmission lines with roughness surface, especially at high frequencies.

ACKNOWLEDGMENT

This work was supported by the National Nature Science Foundation of China (Grant No. 61471293) and the China Scholarship Council (Grant No. 201706285142).

REFERENCES

[1] D. Hollmann, S. Haffa, F. Rostan, and W. Wiesbeck, "The introduction of surface resistance in the three-dimensional finite-difference method in frequency domain," *IEEE Transactions on Microwave Theory and Techniques*, vol. 41, no. 5, pp. 893-895, 1993.

[2] B. Z. Wang, X. H. Wang, and W. Shao, "2D full-wave finite-difference frequency-domain method for lossy metal waveguide," *Microwave and Optical Technology Letters*, vol. 42, no. 2, pp. 158-161, 2004.

[3] B. K. Huang and C. F. Zhao, "Propagation characteristics of rectangular waveguides at tera-hertz frequencies with finite-difference frequency-domain method," *Frequenz*, vol. 68, no. 1-2, pp. 43-49, 2014.

[4] J. P. Donohoe, "A Finite-difference frequency domain solver for quasi-TEM applications," *ACES Journal*, vol. 33, no. 10, pp. 1093-1095, 2018.

[5] Y. J. Zhao, K. L. Wu, and K. K. M. Cheng, "A compact 2-D full-wave finite-difference frequency-domain method for general guided wave structures," *IEEE Transactions on Microwave Theory and Techniques*, vol. 50, no. 7, pp. 1844-1848, 2002.

[6] Q. Li, W. Zhao, Y. J. Zhao, and W. S. Jiang, "Dispersive characteristics analysis of lossy microstrip with 4-component 2-D CFDFD method," *Proceedings-2009 3rd IEEE International Symposium on Microwave, Antenna, Propagation and EMC Technologies for Wireless Communications, MAPE 2009*, Beijing China, pp. 588-592, Oct. 2009.

[7] W. Zhao, H. W. Deng, and Y. J. Zhao, "Dispersion characteristics analysis of lossy coaxial metal waveguide with 4-component compact 2-D FDFD method," *ISAPE 2008-The 8th International Symposium on Antennas, Propagation and EM Theory Proceedings*, Kunming, China, pp. 851-854, Nov. 2008.

[8] W. Zhao, H. W. Deng, and Y. J. Zhao, "Application of 4-component compact 2-D FDFD method in analysis of lossy circular metal waveguide," *Journal of Electromagnetic Waves & Applications*,

vol. 22, no. 17-18, pp. 2297-2308, 2008.

[9] G. Gold and K. Helmreich, "A physical model for skin effect in rough surfaces. *Proceedings of the 7th European Microwave Integrated Circuits Conference*, Amsterdam, The Netherlands, pp. 631-634, Oct. 2012.

[10] G. Gold and K. Helmreich, "Effective conductivity concept for modeling conductor surface roughness," *DesignCon 2014: Where the Chip Meets the Board*, Santa Clara, CA, USA, Jan. 2014.

[11] G. Gold and K. Helmreich, "Surface impedance concept for modeling conductor roughness," *2015. IEEE MTT-S International Microwave Symposium, IMS 2015*, Phoenix, AZ, USA, May 2015.

[12] R. F. Harrington, *Time-harmonic Electromagnetic Fields*. New York: McGraw-Hill, 1961.

[13] B. K. Huang and Q. Jia, "A method to extract dielectric parameters from transmission lines with conductor surface roughness at microwave frequencies," *Progress in Electromagnetics Research M*, vol. 48, pp. 1-8, 2016.

[14] S. Ramo and J. R. Whinnery, *Fields and Waves in Modern Radio*. 2nd Ed., New York: Wiley, 1953.